Ring-Like Nanosheets Standing on Spindle-Like Rods: Unusual ZnO Superstructures Synthesized from a Flakelike Precursor $Zn_5(OH)_8Cl_2 \cdot H_2O$

Biao Liu,[†] Shu-Hong Yu,*[,†] Fen Zhang,[†] Linjie Li,[†] Qiao Zhang,[†] Lei Ren,[‡] and Ke Jiang[†]

Hefei National Laboratory for Physical Sciences at Microscale, Department of Materials Science and Engineering, University of Science and Technology of China, Hefei 230026, P. R. China, and Biomedical Engineering Research Center, Xiamen University, Xiamen 361005, P. R. China

Received: January 9, 2004; In Final Form: February 12, 2004

Unusual ZnO superstructures with nanosheets standing on the backbone of spindle-like rods were synthesized for the first time from a flakelike $Zn_5(OH)_8Cl_2 \cdot H_2O$ precursor under mild solution conditions without using high temperature or any organic molecular templates. The formation of the ring-like nanosheets standing on the spindle is related to the special morphology of the precursor and its solubility, as well as the refluxing reaction conditions. The time dependent shape evolution process and the conductivity measurement of the local reaction solution suggested that the spindle-like ZnO particles were formed at first and then the ring-like nanosheets grew heterogeneously on the backbone of these spindles. The ring-like nanosheets standing on the spindle-like rods was somewhat analogous to nacreous calcium carbonate layers around the columns near the growth tip of a young in red abalone, which could have some implications related with the formation of complex biominerals that exist in nature.

Introduction

Due to the fact that the sizes and shapes of inorganic nanocrystals are important elements which determine their electrical, optical, and some other properties,[1] much effort has been explored for rational controlling over shape, size, dimensionality, and complexity of nanocrystals.[2] ZnO is a potentially useful semiconductor with a direct band-gap of 3.37 eV and a larger excitation binding energy of ∼ 60 meV at room temperature. Since Yang et al. reported ZnO nanowire array nanolasers,[3] synthesis of this material with different forms of controlled nanostructures has been explored widely in recent years. The vapor transport and condensation (CVTC) process[4] is an effective route to synthesize ZnO nanostructures with different morphologies such as nanobelts,[5] nanowire arrays,[6] nanotubes,[7] tetrapods,[8] comblike structures,[9] tower-like structures,[10] and nanowire−nanoribbon junction arrays.[11] More recently, Ren's group has reported novel hierarchical ZnO nanostructures with 6-,4-,2-fold symmetries[12] and nanobridges and nanonails grown on In_2O_3 nanowire cores.[13]

As an alternative synthetic route, a soft chemical method can also generate novel ZnO nanostructures such as nanorods,[14] tubes,[15] highly oriented 2D microrods arrays, or microtubes arrays.[16] Well-defined ZnO nanorods and CdTe nanowires can be self-assembled from individual nanoparticles based on an oriented attachment mechanism[17a] or a spontaneous self-organization process.[17b]

There are many hierarchical nanostructures in nature, and they have acted as fancifully complex functions; however, how to synthesize hierarchical nanostructures is still a big challenge to chemists.[18] Usually, synthesis of hierarchical nanostructures needs high temperatures[9,12] or relies on organic molecular self-assembly, as a template.[19−22]

Recently, Tian et al. have demonstrated an elegant approach for synthesis of biomimetic arrays of oriented helical ZnO nanorods and columns in which citrate was used to retard growth rate of (002) faces under the control of an additive.[23] ZnO crystals with a "stack of pancakes" shape can be growth under the control of the block copolymer poly(ethylene oxide-*block*-styrene)sulfonic acid (P(EO-*b*-SSH)).[24]

Herein, we report a mild solution route to grow novel ZnO superstructures with ring-like nanosheets standing on spindle-like rods without using either high temperature or any organic molecular self-assembly as templates. Such complex morphology was quite analogous to nacreous calcium carbonate layers around the columns near the growth tip of a young in red abalone.[23] The special shaped precursor, its solubility, and the refluxing reaction we adopted were found to play crucial roles in the formation of the unusual complex superstructures.

Experimental Section

I. Preparation of the Precursor. Flake precursor zinc hydroxide chloride hydrate ($Zn_5(OH)_8Cl_2 \cdot H_2O$) can be easily synthesized through a simple and reproducible method. In a typical synthesis, an amount of $ZnCl_2 \cdot 3H_2O$ was added into a beaker and maintained at 80 °C in an electronic oven for 3 h, and it will melt to form an ionic liquidlike solution. Then, 25 mL of the $ZnCl_2$ solution was taken out and added into a beaker, and 0.5 mL of ethylenediamine is slowly dropped into it with magnetic stirring. A white precipitate formed, and then the beaker was kept at 80 °C in an oven for another 12 h. Finally, the white precipitate is filtered off, washed with double distilled water for several times, and dried in a vacuum oven at 60 °C for 3 h.

II. Preparation of the ZnO Superstructures. For the synthesis of the ZnO superstructures, a suitable amount of $Zn_5(OH)_8Cl_2 \cdot H_2O$ (0.066 g) and 55 mL of double distilled water were put into a 100 mL flask. Then 5 mL of ammonia (25 wt

* To whom correspondence should be addressed. E-mail: shyu@ustc.edu.cn. Fax: + 86 551 3603040.
† University of Science and Technology of China.
‡ Xiamen University.

10.1021/jp049881c CCC: $27.50
Published on Web 03/17/2004

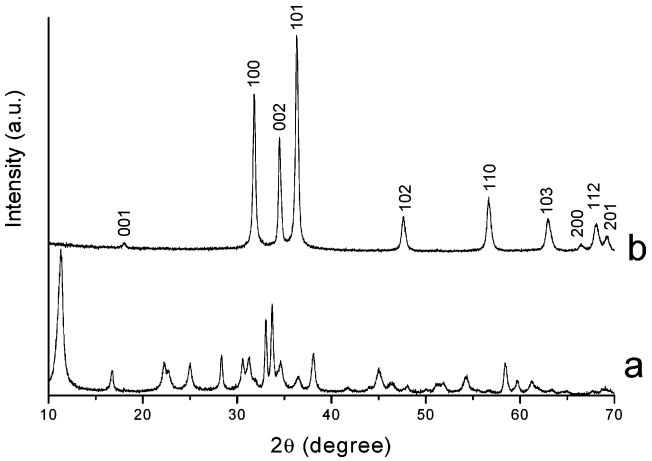

Figure 1. XRD patterns of (a) $Zn_5(OH)_8Cl_2 \cdot H_2O$ and (b) ZnO obtained using $Zn_5(OH)_8Cl_2 \cdot H_2O$ as a precursor.

%) was dropped into it. After that, the flask was maintained in a 120 °C oil bath with refluxing and mild magnetic stirring for 12 h and then cooled to room-temperature naturally. The product is obtained by centrifugation, washed with double distilled water, and dried in a vacuum oven at 60 °C for 3 h.

III. Characterization. The samples were characterized by powder X-ray diffraction (XRD), using a Philips X′Pert PRO SUPER X-ray diffractometer equipped with graphite monochromaticized Cu Kα radiation ($\lambda = 1.541874$ Å), and the operation voltage and current were maintained at 40 kV and 40 mA, respectively. The morphologies, micro- or nanostructure, of the samples were further characterized with field emission scanning electron microscope (FESEM, JEOL JSM-6700F, operated at 10 kV), transmission electron microscopy, and high-resolution transmission electron microscopy performed on a Hitachi (Tokyo, Japan) H-800 transmission electron microscope (TEM) with an accelerating voltage of 200 kV, respectively. The photoluminescence (PL) spectroscopy was carried out at 14 K using a He−Gd laser as the excitation source and a double-grating monochromator connected to a photocounting system. The conductivity of the reaction solution was monitored by a conductance meter DiST WP 3 (Hanna Instruments, Portugal).

Results and Discussion

Figure 1a shows that the product is a pure hexagonal $Zn_5(OH)_8Cl_2 \cdot H_2O$ phase (JCPDS card number 72-0922) with cell constants $a = 6.34$ and $c = 23.64$ Å. Figure 1b shows that the pure ZnO phase can be obtained by refluxing reaction using the flakelike $Zn_5(OH)_8Cl_2 \cdot H_2O$ as a precursor (Figure 2a). In contrast to the standard pattern in JCPDS Card number 36-1451 ($a = 3.246$, $c = 5.209$ Å), a peak with d spacing 4.92 Å appears besides other diffraction peaks, which corresponds to a (001) face, as confirmed by the bright diffraction spots observed in the electron diffraction pattern (Figure 2d), indicating that an unusual structure could exist.

The SEM image in Figure 2b shows an interesting morphology of the produced ZnO particles. Very thin nanosheets are apparently standing on spindle-like rods with a diameter of 300−500 nm and a length of several micrometers (see also Figure 1 in the Supporting Information). The sheets planes are nearly parallel to each other and perpendicular to the length direction of the rods along the [002] direction. The distance between the adjacent sheets is typically about 50−80 nm, which could be due to the strong charge repulsion of two (001) faces. This unique structure with regular spacing sheets is different from the previously reported results about the helical ZnO superstructures[23] or more densely packed lamellae on the backbone of ZnO rods [24] under control either an electrolyte or a block copolymer.

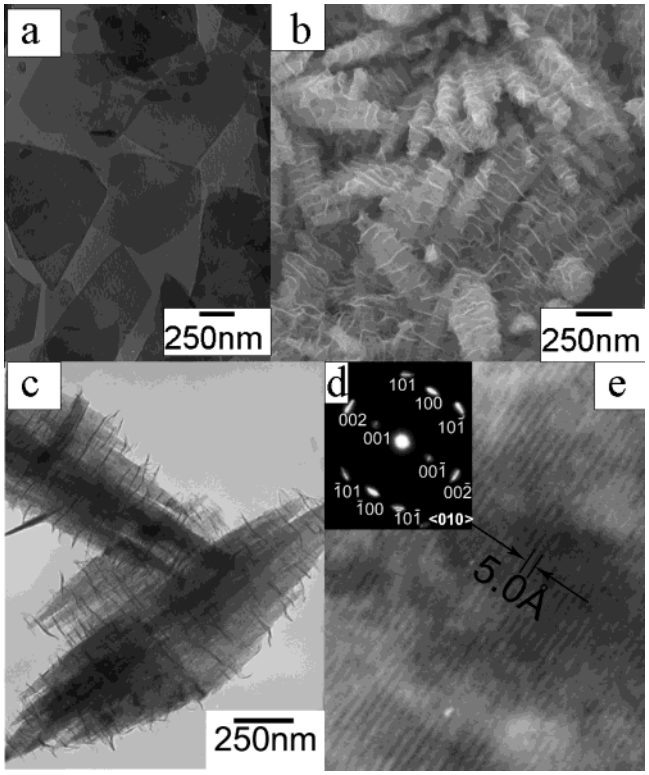

Figure 2. (a) TEM image of the precursor $Zn_5(OH)_8Cl_2 \cdot H_2O$. (b) SEM image of the sample which was obtained by refluxing a solution made of 0.12 mmol $Zn_5(OH)_8Cl_2 \cdot H_2O$, 5 mL of ammonia (25 wt %), and 55 mL of double distilled water in a 120 °C oil bath for 12 h. (c) TEM image of individual spindle-like ZnO hierarchical nanostructure with ring-like nanosheets standing on the rods. (d) The electron diffraction pattern (ED) taken on a single ZnO hierarchical nanostructure. (e) HRTEM image of the structure shown in part c.

The more detailed structural characteristics of the nanostructure were depicted in Figure 2c. The sheets are very thin with thickness of several nanometers. The nanosheets were straightly standing on the backbone of the spindles at the beginning, but they tended to bend somewhat under the continuous irradiation of electron beam. The electron diffraction pattern in Figure 2d taken along the ⟨010⟩ zone axis indicates that the superstructures are single crystals; however, the diffraction spots are slightly tilted, which could be caused by the bending of the nanosheets.

A lattice resolved HRTEM image (Figure 2e) shows that a clear interplanar spacing of about 5.0 Å corresponds to the lattice spacing of (001) planes, indicating that the nanorods grow preferentially along the [001] direction.

To follow the morphology evolution process of the hierarchical nanostructure, the time dependent shape evolution process was examined, and the main results are shown in Figure 3. After the precursor dispersion was refluxed for 40 min, bundles of spindle-like rods formed (Figure 3b). As time goes on, the nanorods start to split into thinner nanorod bundles (Figure 3c). After 4 h, some nanosheets are found to be standing around the surface of the spindles as shown in Figure 3d. The peak corresponding to (001) faces in XRD patterns does not appear until being refluxed for 4 h (data not shown). The results suggest that the presence of (001) peak in the XRD pattern could be relevant to the formation of the superstructures with ring-like nanosheets standing on the rods.

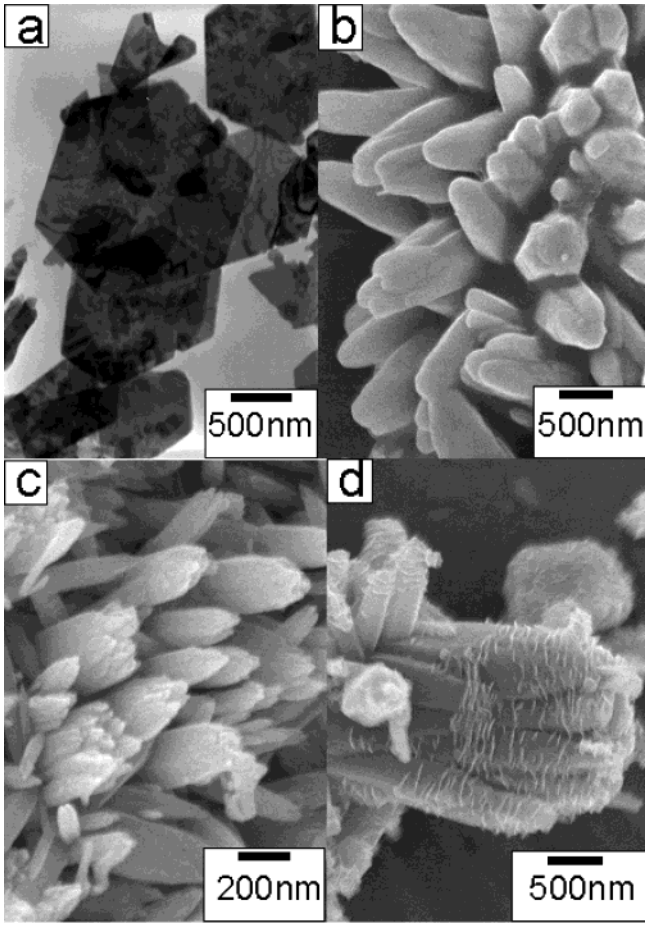

Figure 3. (a) SEM images the morphology of the samples at different stages: (a) the precursor $Zn_5(OH)_8Cl_2 \cdot H_2O$; (b) refluxing for 40 min; (c) refluxing for 2 h; (d) refluxing for 4 h.

The experiments show that the precursor cannot completely dissolve in ammonia solution at room temperature even when it is stirred for long time; however, this precursor could dissolve faster at an elevated temperature. The use of a flakelike precursor and the special solubility of this precursor have an obvious influence on the formation of the hierarchical nanostructure. In contrast, using the same molar amount of ZnO nanorods or other zinc salts such as $ZnCl_2$ instead of the flakelike $Zn_5(OH)_8Cl_2 \cdot H_2O$ precursor with the same molar content of Zn, and keeping other conditions unchanged, no such hierarchical nanostructure can be observed. Even if the amount of $ZnCl_2$ was increased up to 1 mmol, no ZnO phase can be obtained. The results underlie that the special morphology of the precursor and its solubility play crucial roles in the formation of present complex morphology. Especially, the supersaturation state for the formation of the ZnO phase using $Zn_5(OH)_8Cl_2 \cdot H_2O$ can be achieved much earlier than that using other common zinc salts. The conductivity measurement of the solution containing $ZnCl_2$ under the same refluxing condition suggested that no obvious supersaturation leading to ZnO nucleation can be obtained even under high $ZnCl_2$ concentration (see also Figure 2 in the Supporting Information). The results suggested that the special bonding state of Zn^{2+} cations with hydroxy groups will favor the formation of the ZnO phase more easily than other ionic salts.

To further understand the local solution changes during the reaction, the conductivity of the reaction system was followed as shown in Figure 4. The results clearly showed that the conductivity dropped very fast in the early stage, corresponding

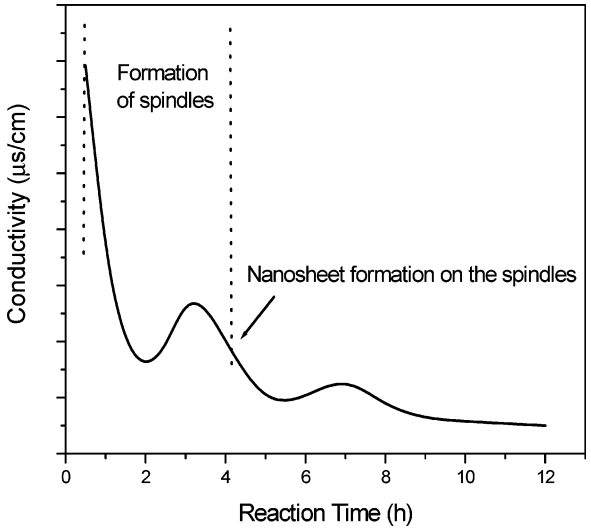

Figure 4. Time dependent conductivity change during the refluxing reaction of a solution made of 0.12 mmol $Zn_5(OH)_8Cl_2 \cdot H_2O$, 5 mL of ammonia (25 wt %), and 55 mL of double distilled water in a 120 °C oil bath for 12 h.

to fast nucleation and precipitation for the growth of the ZnO phase within the initial 2 h. Obviously, the supersaturation for the formation of ZnO is much favored using this precursor which already contains rich hydroxyl groups. The spindle-like ZnO crystals can be formed even after refluxing only for 40 min (Figure 3b). Then, the conductivity of the solution tends to increase during the reaction period of 2−3 h and then decreases until 4.5 h, suggesting a typical dissolution-reprecipitation of the ZnO phase during this stage, accompanying the Ostawald ripening during this period. Later on, the superstructure with ring like nanosheets will form, which was obviously due to the heterogeneous nucleation on the backbone of the spindle-like rods. After the reaction was conducted for 4 h, the conductivity of the solution starts to increase slightly and reaches the highest when the reaction was prolonged until 7 h. Again, the conductivity starts to slightly decrease when the reaction was prolonged further, which could correspond to the similar redissolution and precipitation process for the formation of the ring-like structures as that for the formation of spindles at the first stage. Here, the heterogeneous nucleation growth of the nanosheets on the backbone of the spindles agrees well with that reported on the growth mode of helical ZnO structures formed on the ZnO nanorods [23] and the stacked "pancakes" on the backbone of ZnO rods by a speculated mechanism so-called "a corn on the cob-like structure", where the authors speculated that the single crystalline inner part holds the lamellae together.[24] However, the growth of helical ZnO columns and stacked ZnO pancakes relies on the presence of either organic species or block copolymers.[23,24] In our case, the growth mode of the complex structure did not rely on any organic or polymer additives.

In contrast, the similar reaction was done in a closed environment (hydrothermal process) instead of the refluxing method we adopted here. The morphology of the product was found to be dramatically different from that obtained under refluxing conditions, indicating that the release of ammonia under refluxing conditions also has significant influence on the formation of such complex structures. The regulated pH value during the reaction period through the release of ammonia under refluxing conditions at an elevated temperature can affect the concentration of Zn^{2+} and, thus, the supersaturation of the ZnO phase.

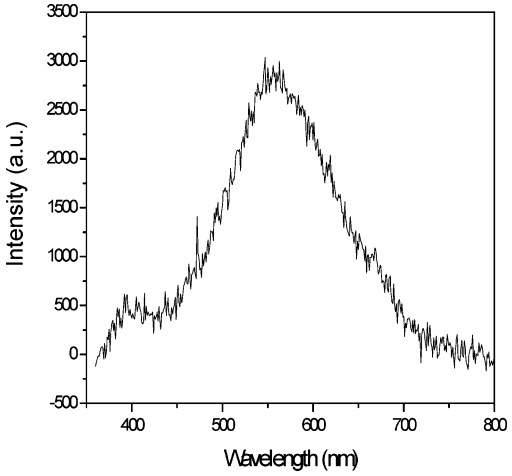

Figure 5. PL spectrum of the complex nanostructure. The excitation wavelength is 325 nm, 14 K.

The formation of the nanosheets on the rods could be due to the secondary nucleation on the backbone of the spindle-like rods. The rough surface of the spindle-like particles was observed at the early stage, which could be due to the redissolution of the ZnO phase. The normal hydrothermal process results in the formation of long ZnO microwiskers instead of the rather complex morphology we observed here, which we will report in due course.

The photoluminescence (PL) spectrum in Figure 5 shows that the hierarchical nanostructure ZnO displays weak ultraviolet emission peaks centered at 395 nm and strong green light emission peaks centered at 550 nm. The emissions at 395 and 550 nm correspond to the near band-edge emission and the deep-level or trap state emission, respectively.[8] The strong green emission and relative weak ultraviolet emission could be related with the special structure feature of the present superstructures, which could contain a large fraction of surface or subsurface oxygen vacancies under the present reaction conditions.

Conclusion

In summary, unusual ZnO superstructures with ring-like nanosheets standing the backbone of spindles were synthesized from $Zn_5(OH)_8Cl_2 \cdot H_2O$ nanosheets by a mild solution route. Several parameters were found to play key roles in the formation of such complex structures, i.e., the special morphology of the precursor and its solubility, as well as the refluxing reaction conditions. The fast supersaturation for the formation of the ZnO phase can be achieved by using the precursor which already has rich hydroxyl groups.

The time dependent shape evolution process and the conductivity measurement of the local reaction solution confirmed that the spindle-like ZnO particles were formed at first and then the ring-like nanosheets grew on the backbone of these spindles. Such an unexpected growth mode could give us some hints about the formation of inorganic materials with an unusual shape and structural complexity, which is somewhat analogous to the minerals such as calcium carbonates that exist in nature.[23] A further understanding of such a complex growth mechanism is ongoing.

Acknowledgment. S.H.Y. is thankful for the special funding support from the Century Program of Chinese Academy of Sciences, the Distinguished Young Fund (Grant No. 20325104), Grant No. 50372065 supported by National Science Foundation of China (NSFC). We thank Prof. Guanzhong Wang of the Department of Physics, University of Science and Technology, for the low temperature PL measurement. We are appreciative of the valuable suggestions from the referee for further revision of this paper.

Supporting Information Available: Image depicting a general view of the produced structure (Figure 1). A plot of the time dependent conductivity change during the refluxing reaction of the solution (Figure 2). This material is available free of charge via the Internet at http://pubs.acs.org.

References and Notes

(1) (a) Lieber, C. M. *Solid State Commun.* **1998**, *107*, 607. (b) Alivisatos, A. P. *Science* **1996**, *271*, 933.
(2) Xia, Y.; Yang, P.; Sun, Y.; Wu, Y.; Mayer, B.; Gates, B.; Yin, Y.; Kim, F.; Yan, H. *Adv. Mater.* **2003**, *15*, 353.
(3) Huang, M. H.; Mao, S.; Feick, H.; Yan, H. Q.; Wu, Y. Y.; Kind, H.; Weber, E.; Russo, R.; Yang, P. D. *Science* **2001**, *292*, 1897.
(4) Yang, P.; Yan, H.; Mao, S.; Russo, R.; Johnson, J.; Saykally, R.; Morris, N.; Pham, J.; He, R.; Choi, H. *Adv. Funct. Mater.* **2002**, *12*, 323.
(5) Pan, Z. W.; Dai, Z. R.; Wang, Z. L. *Science* **2001**, *291*, 1947.
(6) Huang, M. H.; Wu, Y.; Feick, H.; Tran, N.; Weber, E.; Yang, P. *Adv. Mater.* **2001**, *13*, 113.
(7) Hu, J. Q.; Bando, Y. *Appl. Phys. Lett.* **2003**, *82*, 1401.
(8) Yan, H.; He, R.; Pham, J.; Yang, P. *Adv. Mater.* **2003**, *15*, 402.
(9) Yan, H.; He, R.; Johnson, J.; Law, M.; Saykally, R. J.; Yang, P. *J. Am. Chem. Soc.* **2003**, *125*, 4728.
(10) Hu, P.; Liu, Y.; Wang, X.; Fu, L.; Zhu, D. *Chem. Commun.* **2003**, 1304.
(11) Gao, P.; Wang, Z. L. *J. Phys. Chem. B* **2002**, *106*, 12653.
(12) Lao, J. Y.; Wen, J. G.; Ren, Z. F. *Nano Lett.* **2002**, *12*, 1287.
(13) Lao, J. Y.; Huang, J. Y.; Wang, D. Z.; Ren, Z. F. *Nano Lett.* **2003**, *3*, 235.
(14) Andrés-Vergés, M.; Mifsud, A.; Serna, C. J. *J. Chem. Soc., Fraday Trans.* **1990**, *86*, 959.
(15) Zhang, J.; Sun, L.; Liao, C.; Yan, C. *Chem. Commun.* **2002**, 262.
(16) (a) Vayssieres, L. *Adv. Mater.* **2003**, *15*, 464. (b) Vayssieres, L.; Keis, K.; Lindquist, S. E.; Hagfeldt, A. *J. Phys. Chem. B* **2001**, *105*, 3350. (c) Vayssieres, L.; Keis, K.; Hagfeldt, A.; Lindquist, S. E. *Chem. Mater.* **2001**, *13*, 4395.
(17) (a)Pacholski, C.; Kornowski, A.; Weller, H. *Angew. Chem., Int. Ed.* **2002**, *41*, 1188. (b) Tang, Z. Y.; Kotov, N. A.; Giersig, M. *Science* **2002**, *297*, 237.
(18) Cölfen, H.; Mann, S. *Angew. Chem. Int. Ed.* **2003**, *42*, 2350.
(19) (a) Brunsveld, L.; Zhang, H.; Glasbeek, M.; Vekemans, J. A. J. M.; Meijer, E. W. *J. Am. Chem. Soc.* **2000**, *122*, 6175. (b) Bockstaller, M.; Köhler, W.; Wegner, G.; Vlassopoulos, D.; Fytas, G. *Macromolecules* **2000**, *33*, 3951. (c) Guo, L.; Ji, Y. L.; Xu, H.; Simon, P.; Wu, Z. *J. Am. Chem. Soc.* **2002**, *124*, 14864.
(20) (a) Mann, S. *Angew. Chem., Int. Ed.* **2000**, *39*, 3392. (b) Dujardin, E.; Mann, S. *Adv. Mater.* **2002**, *14*, 775.
(21) Yu, S. H.; Antonietti, M.; Cölfen, H.; Hartmann, J. *Nano Lett.* **2003**, *3*, 379.
(22) Shi, H.; Qi, L.; Ma, J.; Cheng, H. *J. Am. Chem. Soc.* **2003**, *125*, 3450.
(23) Tian, Z. R.; Voigt, J. A.; Liu, J.; Mckenzie, B.; Mcdermott, M. J. *J. Am. Chem. Soc.* **2002**, *124*, 12954.
(24) (a) Taubert, A.; Palms, D.; Glasser, G. *Langmuir* **2002**, *18*, 4488. (b) Taubert, A.; Kubel, C.; Martin, D. C. *J. Phys. Chem.* **2003**, *107*, 2660.